Computer Simulation in Designing Electrostatic Optics for Space Plasma Experiments

J. P. McFadden and C. W. Carlson

Space Sciences Laboratory, University of California, Berkeley

Abstract. The design of new experiments is an art that combines innovative concepts, simulations, mechanical design, assembly, test and calibration. Although an instrument's development may proceed linearly through these steps, more often the design evolves through a complicated processes of trade offs. Optimizing practical features (ease of assembly, compactness, low mass, low cost) is often at odds with the design concept (complicated optics, high sensitivity). Balancing these design considerations often drives the experiment away from the original concept, but produces a much more robust, constructible instrument. An essential tool for analyzer design is a set of computer simulation programs that allow optics concepts to be tested prior to construction. These programs allow the scientist or engineer to quickly test new ideas without the cost of developing a prototype. This paper outlines computer codes used to design electrostatic optics for low energy plasma detectors. A number of features that enhance the usefulness of these programs are also described. As an example of analyzer design, the development of the electrostatic optics for the Cluster CIS-1 mass spectrometer is described.

INTRODUCTION

Until the last 10-15 years, the development of space plasma detectors relied on analytic calculations of electrostatic and magnetic optics. Optics designs were limited to fairly straightforward geometries such as spherical or cylindrical electrostatic analyzers (ESAs) that afford themselves to analytic calculations [*Paolini and Theodoridis*, 1967; *Theodoridis and Paolini*, 1968]. Sophisticated optics were sometimes selected, such as second order focusing in magnetic spectrometers [*Coplan et al.*, 1984], to perform high resolution measurements. Once the optics were selected, prototypes would be constructed to test the design, often followed by modifications to correct the optics for fringing fields or nonuniform magnets, which were beyond the scope of the analytic calculation methods. Modifications would often be based on an intuitive understanding of the optics or through trial and error. Once the prototype was optimized, flight units would be constructed and calibrated. The calibration produced the best measurements of the analyzer response, but would often be incomplete due to limitations of calibration facility.

More recent analyzer designs do not readily afford themselves to analytic calculations. Even a fairly simple concept such as the "top-hat" analyzer [*Carlson and McFadden*, this volume; *Carlson et al.*, 1983] has a number of design parameters. An analytic characterization has been performed [*Michael*, 1980], however mechanical details in an actual design may be more complex than the analytic model. In order to design and characterize more sophisticated optics, computer codes have been developed to ray trace particles through the analyzers, eliminating development costs associated with prototypes.

This paper describes the computer programs developed by the authors to design electrostatic optics for low energy plasma detectors. It is not intended to be a comprehensive article on code development or optimization. The intention is to summarize the main features that were required of the simulation code and to present an example of the design

Measurement Techniques in Space Plasmas: Particles
Geophysical Monograph 102

procedures used to construct space plasma analyzers. The paper begins with an overview of simulation codes followed by an in depth description of the development of the Cluster CIS-1 optics.

OVERVIEW OF COMPUTER CODES

Three main programs were used to perform electrostatic optics design and testing: 1.) a Laplace equation solver (LAP) to calculate the potential solution on a finite grid mesh, 2.) a particle trajectory solver (TRJ) to ray trace particles through the potential grid generated by LAP, and 3.) graphical routines (GRAPH) to plot and manipulate the trajectory data obtained from TRJ. These codes were developed in 2-D (r,z) and 3-D (r,z,θ) cylindrical coordinate systems to reflect the symmetry found in spherical and toroidal ESAs and Time-Of-Flight (TOF) detectors. In contrast, Carlson et al. (1983) used a 2-D spherical coordinate system to map the top-hat entrance aperture, then used a combination of 3-D ray tracing near the aperture and analytic calculation of trajectories between the hemispheres.

The LAP program employs only Dirichlet boundary conditions and an iterative solution based on the diffusion equation and overrelaxation. *Potter* [1973] compares a number of iterative methods and shows that those that include overrelaxation schemes converge the fastest. We tried using variations on both the successive overrelaxation (SOR) and Chebyshev methods, but found no significant improvement over simple fixed overrelaxation coefficients for our geometries. Coefficients from 1.7 to 1.9 worked well for spacing between different potential surfaces from 15 to 60 grid points, which is similar to that reported by *Sablik et al.* [1988]. Since overrelaxation schemes tend to favor potential diffusion in the direction of the grid stepping during an iteration, we ran the inner and outer grid stepping loops in reverse order on alternate iterations (not the AID method) to increase convergence by symmetrizing the diffusion. A modified iteration formula near coordinate singularities was also required.

Other useful features of the LAP program include array doubling, adding, and scaling, "DXF" file importation, and periodic and nonuniform boundary specification. A factor of 2 increase in grid resolution will increase the LAP calculation time by approximately 2^{N+1}, where N (2 or 3) is the coordinate system dimension. Starting with a coarser array and using array doubling reduces the increased calculation time to only about 2^{N-1}, since only a small number of iterations are required in the doubled array. The LAP program is able to add and scale arrays with equivalent boundaries but different potentials in order to allow rapid changes in the relative potentials. A program was written to convert a "DXF" file into a set of boundary condition commands to allow mechanical drawings developed on CAD systems to be directly imported. The grid's outer boundaries are periodic when possible to take advantage of symmetry. Linear boundaries can be specified with different potentials at each end, and with linear or power law interpolation in between. The LAP program can also correct the potential on curved boundaries to account for finite grid size. The user specifies both the potential and normal gradient at the surface, not to overspecify the boundary condition, but to correct the potential of boundary points not lying exactly on the specified surface. The potential gradient can often be estimated fairly accurately, producing a first order correction near the surface that reduces errors in the ray tracing.

The TRJ program is used to ray trace particles through the potential grid generated by LAP. A number of ray tracing algorithms exist (Runge-Kutta, Leap-frog, etc.) which require different levels of complexity for the ray-tracing algorithm and offer some variations in speed and accuracy. Most of the code developed by the authors used second order calculations of both "dx" and "dv" at a single time step to simplify the algorithm. To determine if a particle strikes a boundary, a boundary testing algorithm is run at each trajectory step. A simple 2-D (3-D) algorithm tests if the nearest two (four) grid points are boundaries, and if so was the previous position on the other side of the line (plane) defined by the points. For this routine to work it is important that the particle move less than 1 grid spacing each iteration.

The ray tracing routine uses a fixed "ds" each iteration rather than a fixed delta time "dt", where "ds" is a fraction of the grid spacing, to limit particle motion. Errors are introduced by discontinuities in the locally calculated potential caused by finite grid size. These errors can be reduced by increasing the number of grid points used to calculate the local field or by functional fitting (cubic spline fits), however these methods generally increase computational time and complicate calculations near boundaries. We chose instead to monitor the errors in the total particle energy and found that the cumulative error was small for our simulations. The code was also occasionally run with explicit energy conservation at each step to test for consistency and to look for regions where grid resolution was inadequate. Virtually identical results were obtained whether or not energy conservation was explicit.

The TRJ program has an interactive mode and batch mode. The interactive mode allows projection of the particle trajectories onto any surface with constant r, z, or θ, and includes boundaries that pass through the selected surface. Initial conditions for the particles can be specified with an "input file" or with a single initial condition, step size, and number of trajectories. An "output file" of initial and final position-velocity vectors is generated with the same format as the "input file", allowing the output of one ray tracing set as the input to another ray tracing. Output file vectors include only those rays that pass through a specified surface. A trajectory "timer" is also incorporated into the TRJ output file, by summing the "dt"s of the trajectory between two surfaces, and is useful for designing TOF optics.

The batch mode for TRJ is used to characterize an analyzer by finding the total throughput with a finite resolution

(dr, dv). Rather than run a large 4-volume in the 6-D initial condition phase space and obtaining a low throughput (typically 5%), we developed an algorithm that only ran nearest phase space neighbors of throughput rays. After specifying a single initial condition, all throughput trajectories in a contiguous region of initial condition phase space are found. The ratio of throughput trajectories to total trajectories for this algorithm is >50% for common analyzer designs and ~30,000 total trajectories.

A similar scheme involving mapping only the surface of the initial condition phase space has also been used [*Woodliffe and Johnstone*, this volume]. This scheme has the potential to reduce the number of trajectories needed, however the phase space volume of throughput trajectories is often a thin extended volume so a similar number of trajectories may be required to characterize the surface and volume. The surface mapping algorithm also has the following drawbacks. First, the surface of initial conditions consists of those rays that pass near a boundary, thus they are the trajectories most prone to error due to finite grid size. Second, since surface mapping does not generate final position-velocity vectors for all throughput trajectories, it will not generate an "output file" that can be used as an "input file" for another tracing. Third, having the final position-velocity vectors of all throughput trajectories allows the "GRAPH" program (below) to plot analyzer response at the analyzer exit and to perform additional manipulation on the trajectory data such as the response to an exit collimator.

A "GRAPH" program was developed that displays and manipulates the "output files" generated by TRJ. The primary use of this program is to allow direct comparison of simulation with instrument testing and calibration. The GRAPH routines plot averages or slices through the distribution of initial or final conditions, generating line or contour plots. Fitting routines are included to allow comparison of analyzer energy constants, energy width, angular width, etc. The routines also determine analyzer geometric factor, which may have to be slightly corrected for finite grid size. The GRAPH program permits both entrance and exit collimation specification to allow one to quickly tweak the analyzer response without rerunning the entire TRJ simulation. The program also generates plots of the distribution of particles at different initial or final positions, assuming field free propagation, which are useful in locating focal points.

Other specialized plotting routines were developed to determine the uniformity of sampling with spacecraft spin required to cleanly resolve the solar wind density for the WIND 3-D Plasma Experiment, to characterize a set of equally spaced collimation slits on the 360° FOV Mars Observer Electron Reflectometer, and determine variations in the angle between the particle velocity and microchannel plate (MCP) bias angle which affects MCP efficiency [*Gao et al.*, 1984]. This last simulation showed that a single 360° MCP ring would not be appropriate for top-hat detectors, but that 180° half rings would have only small efficiency variations. Finally a routine was developed to convolve an analyzer's response with a two species (proton and alpha), two temperature (parallel and perpendicular to **B**), drifting distribution to determine how well experiments could resolve the narrow solar wind beam.

DESIGN OF THE CLUSTER CIS-1

Instrument design should begin with a definition of the science requirements. For a particular investigation the experiment must be sensitive over a range of fluxes, have an energy and angular response capable of resolving features of the particle distribution function, and have high signal to noise ratios. Once these requirements are defined, development of the experiment can proceed by selecting a design concept and searching the parameter space of the concept. If the basic optics and mechanical design are not known, the main design effort is to develop the concept to a smaller parameter space with similar optics and mechanical configurations. Optics simulations and mechanical design should proceed in parallel, otherwise one will likely develop optics that are either difficult or impossible to construct. The design normally begins with simulations of rough mechanical concepts to test and refine the optics, followed by a more complete mechanical design. Simulation is then used to test changes in the optics due to mechanical requirements and to test for expected machining tolerances.

An example of instrument design is illustrated by the development of the CIS-1 analyzer [*Reme et al.*, 1993] for the four Cluster Spacecraft. The science requirements were for a large geometric factor mass spectrometer with a 4π steradian field of view, one spin resolution, large dynamic range in sensitivity to resolve solar wind to lobe plasma fluxes, 0-40 keV energy range, and mass resolution of the primary magnetospheric and solar wind components (H+, He+, He++, O+). The requirement for a large geometric factor effectively ruled out mass spectrometers that utilized magnets within the experiment mass constraints. Instead a design was chosen that combines a Time-Of-Flight (TOF) particle detector with a top-hat ESA, thereby resolving both energy per charge and velocity. This analyzer has the large effective geometric factor of the ESA, reduced only by TOF efficiency (30%-50%). This can be 1-2 orders of magnitude larger than designs using magnets since magnet designs require field-of-view constraints and often only resolve one mass at a time. The energy range and mass resolution required the design to post- accelerate ions between the ESA and TOF by 25 kV. An ESA of the top-hat type was chosen to satisfy the 4π steradian field of view each spin. A large dynamic range in sensitivity was accomplished by reducing the geometric factor on half of the analyzer using a pinhole array attenuator. Finally, dynamic range requirements that the experiment resolve both narrow intense beams (solar wind) and tenuous fluxes (lobes) proved too difficult for a single experiment, so a second,

small dedicated ESA (CIS-2) was chosen to handle the intense narrow solar wind proton flux.

Once the design approach was selected, a preliminary mechanical design was sketched in an attempt to develop optics that would be easy to construct and service. A clean interface between the ESA and TOF was adopted to avoid complicated mechanical assembly and to allow both sections to be independently constructed, tested and calibrated.

The initial design effort concentrated on developing the TOF section. The TOF detector consists of a 25 kV post-ESA acceleration region, a thin carbon foil that produces secondary electrons, a drift region between the foil and ion detector, an ion detector which produces the "Stop" signal, and an electron detector which collects the foil electrons and generates the "Start" signal. A simple modular approach was attempted that would contain a single MCP detector plane for both "Start" and "Stop" particles, a drift optics section which would focus ions and electrons onto the plane, and a single internal voltage to collect the secondary electrons. Figure 1 shows a pair of simulations that have been combined into a single figure to show the basic ion and electron trajectories through the ESA and TOF.

A 2-D simulation code in cylindrical coordinates (r,z) was initially used to investigate optics needed to collect foil electrons. Internal voltages were assumed to be small (about 2 kV) relative to the 25 kV supply, so that ion optics would be relatively unaffected. The requirement was that foil electrons with arbitrary initial velocities and energies up to 20 eV, or 1% of the applied voltage, would all be focussed to the "Start" detector. Azimuthal confinement of the electrons was required to minimally defocus the 22.5° resolution requirement in the image plane. Scattering of the ions in the foil made their choice for azimuthal angle imaging unattractive. Additional requirements were a foil width of at least 6 mm centered at a 75 mm radius, and a 40 mm ion drift. The lower portion of Figure 1 shows a 3-D simulation where electrons with initial energies of 1% of the applied voltage are emitted at 80° from normal and focussed onto the "Start" detector. Electrons as they leave the foil are focussed by the curved potential surfaces next to the foil, then accelerated to about half the applied voltage and deflected to the "Start" MCP. Roughly 30 2-D simulations were required to develop a proper geometry, which was found to be sensitive to the initial lens near the foil but not sensitive to the deflection geometry. The range of electron transit times from the foil to "Start" detector was calculated and found to be an acceptable error in the TOF. Other considerations that influenced the design included the elimination of ion trajectories that could reach the "Start" MCP, the baffelling of the surfaces to reduce internal scattering, and optics that prevented secondary electrons generated on any other internal surfaces from reaching the "Start" or "Stop" MCP. A 2-D design was achieved that satisfied all the requirements except for the minimal azimuthal spreading of electrons.

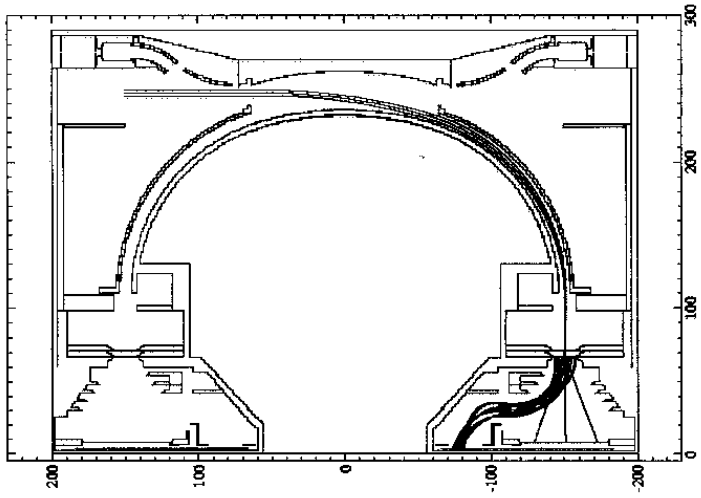

Figure 1. Ray tracing of ions and foil electrons through the Cluster CIS-1 mass spectrometer. Ions are selected for energy/charge by the toroidal ESA, are post-accelerated to 25 keV, pass through a thin carbon foil, and strike the "Stop" MCP detector. All foil electrons with up to 20 eV energy are collected on the "Start" MCP when a 2 kV internal deflection voltage is used.

In order to achieve foil electron imaging with 22.5° resolution at the "Start" detector, a 3-D cylindrical simulation (r,z,θ) was used to refine the optics. It was hoped that small adjustments in the boundary conditions near the 22.5° boundaries would produce the desired focussing. The 3-D simulation required a much larger array but took advantage of the 16 fold symmetry by calculating the potential for only one 22.5° sector and using periodic boundary conditions. The lower portion of Figure 2 shows the results of the simulation. A small protrusion at the 22.5° boundaries of the foil and another near the midpoint of the trajectories were found to provide excellent focussing of the electrons onto the "Start" plane. Both of these features were easy to incorporate into the mechanical design.

Once the design of the TOF optics was complete, the electrostatic analyzer optics were examined. A toroidal analyzer design was chosen to push the imaging of the ion focal plane past 90° and into the region between the analyzer and the foil (upper portion Figure 2). Toroidal designs contain a pair of deflection plates with an r-z radius of curvature of "R_1" and the origin of the curvature located off the z-axis at a distance "R_0" (see Figure 3). By selecting various ratios of R_0/R_1, one can adjust the azimuthal focal point. In the limit $R_0 \rightarrow 0$ one obtains a hemispherical analyzer, and when $R_0 \rightarrow \infty$ one obtains a cylindrical analyzer with no azimuthal focussing. Ideally the ion focal point should be at the foil, however the focussing is a function of energy since low energy ions leaving the analyzer are strongly affected by the 25 kV potential. In order to optimize the ion beam focussing at the foil for all energies (0-40 keV) with 25 kV post-acceleration, the analyzer focal point was located approximately one-third of the distance between the analyzer exit and foil.

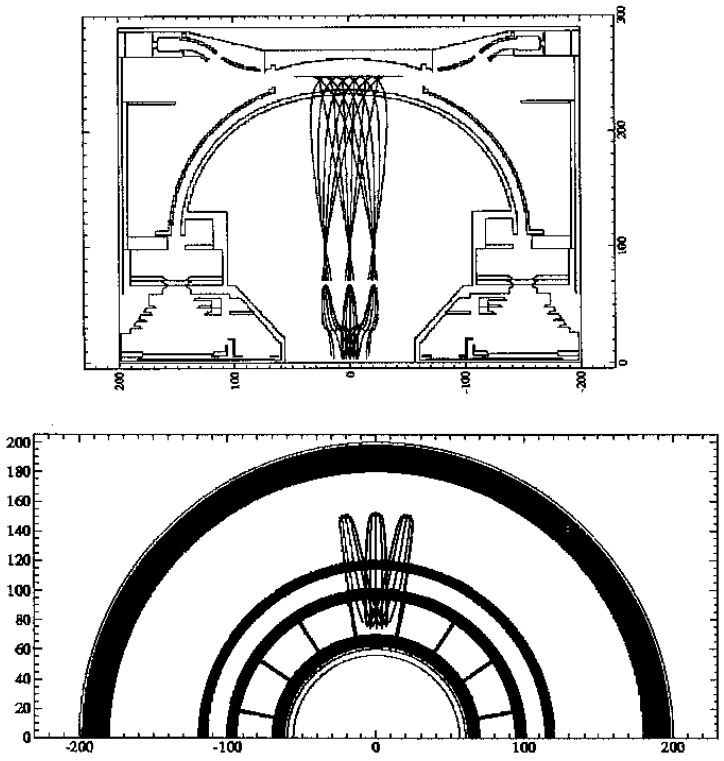

Figure 2. Ray tracing of ions (upper plot) shows the toroidal analyzer's focal point is below the analyzer exit. Ray tracing of secondary electrons produced on the TOF foil (lower section of upper plot and lower plot) shows the 3-D imaging of electrons onto the "Start" detector.

The design of the toroidal analyzer involves a large number of parameters. A toroidal design that preserved the curved "top-hat" was chosen rather than a "flat-topped" [*Young et al.*, 1988] design to minimize U.V. scattering into the instrument by flat surfaces. A design philosophy was chosen that transitions from toroidal to spherical in the top-hat region by smoothly matching boundary conditions (position and slope) at the interface. The geometry is shown in Figure 3, which has radii R_0, R_1, R_2, and $dR_1 = (R_2\text{-}R_1)$ to determine the toroidal section, and radii R_3, R_4, and $dR_3 = (R_4\text{-}R_3)$ to determine the spherical section. This design has a smooth transition to a hemispherical analyzer as $R_0 \rightarrow 0$. This approach simplifies the design since setting $dR_3 = 2dR_1$ produces a nearly planar FOV. The opening angle Θ_1 can then be chosen to make second order corrections for a planar FOV. It should be noted that a "curved top-hat" section produces an azimuthal focal point that is not as distant as a "flat-top" analyzer, however from the limited number of simulations that we have performed, the astigmatism (sharpness of the focal point) appears better for this design.

To design the CIS-1 toroidal ESA, a number of simulations were performed adjusting R_0 to obtain the optimal azimuthal focal point, and adjusting Θ_1 to obtain a planar response. Each design change requires a full simulation of the energy and angle response. Collimation is then introduced to eliminate unwanted trajectories that produce high energy tails in the energy response or to symmetrize the angle response. Figure 4 shows the energy and angle response of the final design. The analyzer geometric factor is 0.06 cm^2-sr-eV/eV, energy resolution is dE/E=0.15 FWHM, and $d\alpha$ is 6° FWHM.

Once the toroidal analyzer design was complete, a set of simulations with various ratios of hemisphere voltage to post-acceleration voltage were performed to determine the ion focussing at the foil and thereby the foil width required in the radial direction. These simulations showed that even the 40 keV ions would all hit within the planned 6 mm foil radial width. Concern arose that secondary electrons produced on the analyzer side of the foil and accelerated to 25 kV would generate x-rays or sputtered ions, possibly producing a cascade with positive feedback. This problem was avoided by using simulations to design the foil mounting to focus these secondary electrons back into the analyzer thereby preventing cascade. Later a second grid with the same geometry was added above the foil to eliminate field emitted electrons from small tears that occasionally developed in the foils [*Moebius et al.*, this volume].

Once the basic optics designs were complete, prototypes were developed for the TOF. During the design phase, improvements in the electronics showed that a 30 mm ion drift was adequate in the TOF. The prototype mechanical design was changed from the simulation design by shortening the ion drift region to 30 mm and modifying optics near the foil where the simulation had shown that the design was sensitive. Unfortunately these changes were made without confirmation by simulation and it was found that the foil

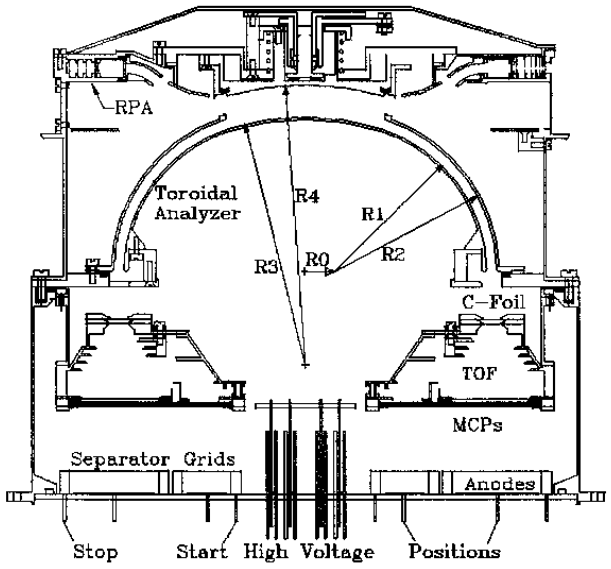

Figure 3. Mechanical drawing of the Cluster CIS-1 ESA followed by the TOF detector. The ESA has a toroidal geometry to push the ion focal point past the analyzer exit. The upper set of deflectors and grids allow the ESA to be run as an RPA.

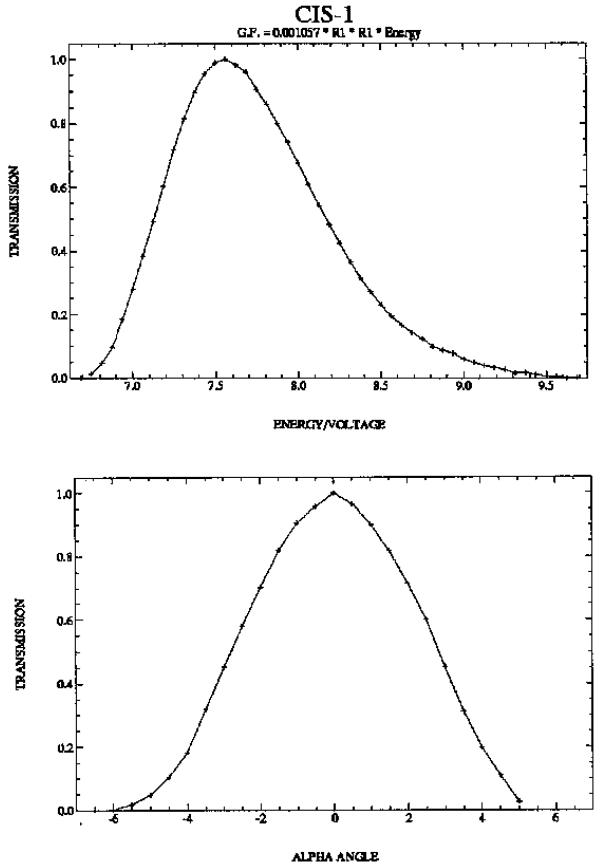

Figure 4. Energy (4a) and Angle (4b) response of the CIS-1 analyzer from ray tracing simulations.

electron imaging was severely degraded in the prototype. A handful of additional simulations were required to correct the optics, and modifications to the prototype were made.

Before a prototype of the toroidal ESA could be built, the design of a Retarding Potential Analyzer (RPA), as part of the main entrance aperture, had to be completed. Inclusion of the RPA was for a secondary science requirement of measuring cold ions. A discussion of the RPA optics design, which required numerous simulations but did not impact any of the design features described above, can be found in *McCarthy and McFadden* [this volume]. Additional discussions of CIS-1 can be found in *Moebius et al.* [this volume].

SUMMARY

We have presented an outline of the electrostatic optics programs that were developed at the University of California, Berkeley to aid the design of low energy, space plasma analyzers. We have included a description of the main programs and their features. As an example of analyzer design, a detailed description of the development of the electrostatic optics for the Cluster CIS-1 mass spectrometer is included. It is hoped that this presentation will be a useful example and outline to those developing space plasma experiments.

Acknowledgments. We would like to thank J. Clemmons, D. Curtis, N. Danner, and D. Larson for useful programming discussions and help in developing the code. The realization of the Cluster CIS detectors was the combined effort of individuals (see *Rème et al.*, 1993) from several institutions. This work was funded in part by NASA Contracts NAG5-959, NGL-05-033-017, NAS5-30366, and NAS5-31283 and subcontract UW/376990 at UC Berkeley.

REFERENCES

Carlson, C. W., D. W. Curtis, G. Paschmann, and W. Michael, An Instrument for Rapidly Measuring Plasma Distribution Functions with High Resolution, *Adv. Space Res.*, *2*, 67-70, 1983.

Carlson, C. W., and J. P. McFadden, Design and Applications of Imaging Particle Instruments, *Geophysical Monograph*, this volume.

Coplan, M. A., J. H. Moore, R. A. Hoffman, Double Focusing Ion Mass Spectrometer of Cylindrical Symmetry, *Rev. Sci. Instrum.*, *55*, 537-541, 1984.

Gao, R. S. , P. S. Gibner, J. H. Newman, K. A. Smith, and R. F. Stebbings, Absolute and angular efficiencies of a microchannel-plate position-sensitive detector, *Rev. Sci. Instrum.*, *55*, 1756- 1759, 1984.

Lin, R. P., K. A. Anderson, S. Ashford, C. Carlson, D. Curtis, R. Ergun, D. Larson, J. McFadden, M. McCarthy, G. K. Parks, H. Reme, J. M. Bosqued, J. Coutelier, F. Cotin, C. D'Uston, K.-P. Wenzel, T. R. Sanderson, J. Henrion, J. C. Ronnet, and G. Paschmann, A Three-Dimensional Plasma and Energetic Particle Investigation for the Wind Spacecraft, *Space Sci. Rev.*, *71*, 125-153, 1995.

McCarthy, M., and J. P. McFadden, Measurements of 0-25 eV Ions with a Retarding Potential Analyzer on the Cluster Ion Spectroscopy Experiment, Geophysical Monograph, this volume.

Michael, W., Untersuchungen an Einem Plasmaanalysator mit 360° Offnungswinkel, Technische Universitat Munchen, Diplomarbeit, 1980.

Moebius, E., L. M. Kistler, M. Popecki, K. Crocker, M. Granoff, Y. Jiang, E. Sartori, V. Ye, Reme, H., J. A. Sauvaud, A. Cros, C. Aoustin, T. Camus, J.-L. Medale, J. Rouzaud, C. W. Carlson, J. McFadden, D. Curtis, H. Heetderks, J. Croyle, C. Ingraham, E. C. Shelley, D. Klumpar, E. Hertzberg, B. Klecker, M. Ertl, F. Eberl, H. Kaestle, E. Kunneth, P. Laeverenz, E. Seidenschwang, G. K. Parks, M. McCarthy, A. Korth, B. Grawe, H. Balsinger, U. Schwab, and M. Steinacher, The 3-D Plasma Distribution Function Analyzers With Time-of-flight Mass Discrimination for CLUSTER, FAST, and Equator-S, *Geophysical Monograph*, this volume.

Paolini, F. R., and G. C. Theodoridis, Charged Particle Transmission through Spherical Plate Electrostatic Analyzers, *Rev. Sci. Instrum.*, *38*, 579-589, 1967.

Potter, D., Computational Physics, Wiley, London, 1973.

Reme, H., J. M. Bosqued, J. A. Sauvaud, A. Cros, J. Dandouras,

C. Aoustin, Ch. Martz, J. L. Medale, J. Rouzaud, E. Moebius, K. Crocker, M. Granoff, L. M. Kistler, D. Hovestadt, B. Klecker, G. Paschmann, M. Ertl, E. Kunneth, C. W. Carlson, D. W. Curtis, R. P. Lin, J. P. McFadden, J. Croyle, V. Formisano, M. DiLellis, R. Bruno, M. B. Bavassano-Cattaneo, B. Baldetti, G. Chionchio, E. G. Shelley, A. G. Ghielmetti, W. Lennartsson, A. Korth, H. Rosenbauer, I. Szemerey, R. Lundin, S. Olsen, G. K. Parks, M. McCarthy, and H. Balsinger, in Cluster: Mission, Payload and Supporting Activities esa SP-1159, e. W. R. Burke, p. 133, European Space Agency, Paris, 1993.

Sablik, M. J., G. Golimowski, J. R. Sharber, and J. D. Winningham, Computer simulation of a 360° field-of-view "top-hat" electrostatic analyzer, *Rev. Sci. Instrum., 59*, 146-155, 1988.

Theodoridis, G. C., and F. R. Paolini, Charged Particle Transmission through Cylindrical Plate Electrostatic Analyzers, *Rev. Sci. Instrum., 39*, 326-331, 1968.

Woodliffe, R. D., and A. D. Johnstone, The use of numerical simulation in the design of the Cluster/Peace "Top-Hat" analyzer electron optics, *Geophysical Monograph*, this volume.

Young, D. T., S. J. Bame, M. F. Thomsen, R. H. Martin, J. L. Burch, J. A. Marshall, and B. Reinhard, 2π-Radian Field-of-View Toroidal Electrostatic Analyzer, *Rev. Sci. Instrum., 59(5)*, 1988.

Carlson, C.W. and McFadden, J.P., Space Sciences Laboratory, University of California, Berkeley, 94720.